Maritime Technology and Society
Vol. 4(3): 253-264, October 2025
https://doi.org/10.62012/mp.vi.46023

Regular Research Article

Redesign of the Graving Dock Gate Structure Using Finite Element Method to Achieve a More Optimal and Efficient Construction

Indah Melati Suci [1]*, Alamsyah[2], Samsu Dlukha Nurcholik[2], Martinus[2], and Muhammad Zubair Muis Alie [3]

[1] Department of Ocean Engineering, Kalimantan Institute of Technology, Balikpapan, Indonesia
[2] Department of Naval Architecture, Kalimantan Institute of Technology, Balikpapan, Indonesia
[3] Departement of Ocean Engineering, Engineering Faculty, Hasanuddin University, Indonesia
* Correspondence author: indah.suci@lecturer.itk.ac.id ; Tel.: +62-8215-4793-309

Abstract: The graving dock gate is a critical structure in shipyard facilities, functioning as a barrier to retain seawater during docking operations. Its performance determines operational efficiency and safety. At PT Barokah Galangan Perkasa, the existing gate design was found to be excessively heavy, exceeding the required load capacity and preventing it from floating during low-water conditions. This inefficiency highlighted the need for redesign to achieve a balance between structural strength and weight efficiency. The existing gate dimensions are 46 m in length, 3 m in breadth, and 7.32 m in depth. The redesign applied the Finite Element Method (FEM) using ANSYS Mechanical APDL for structural strength analysis, supported by 3D modeling in AutoCAD and SketchUp. A parent design approach was used to define initial dimensions, while modifications focused on reducing weight by adjusting plate thicknesses and steel profiles according to BKI (2009) standards. The structural model was subjected to meshing, loading, and boundary condition simulation to evaluate stress distribution, deformation, and safety factors. Results showed that the redesigned gate, constructed with KI-A36 steel, withstood a maximum von Mises stress of 335.44 MPa, well below the material's yield strength. The maximum deformation was 2.657 mm, within acceptable limits. Notably, the redesign reduced weight by 25.49% (from 187.96 tons to 140.04 tons) without compromising integrity. These improvements are expected to enhance operational performance, maneuverability, and cost efficiency while maintaining safety standards.

Keywords: Graving Dock; Gate Redesign; Finite Element Method; Structural Optimization; Weight Reduction.

1. Introduction

The graving dock is one of the essential supporting facilities in a shipyard. It is a large basin located by the seaside, and its construction generally consists of side walls, a floor, a front wall, and a gate that is directly exposed to seawater. Every graving dock must have a gate that allows ships to enter and exit during the docking or undocking process [1]. The gate serves as a crucial structure to prevent seawater from entering the dock. In general, there are several types of graving dock gates, including flap gates, floating caisson gates, intermediate gates, sliding and rolling caisson gates, mitre gates, and others [2].

The operational process of a graving dock begins when a ship is about to enter: the gate is opened, and once the ship is inside, the gate is closed. After closing the gate, seawater inside

Received 2025-07-31; Accepted 2025-09-15; Published 2025-10-12

the dock is pumped out until the basin is dry [3]. The pressure of the seawater outside the dock presses against the gate, effectively locking it in place. Work on the ship is then carried out in the dry dock. Upon completion, the dock is refilled with seawater, balancing the pressure inside and outside the dock. This balance releases the lock, allowing the gate to move freely. The graving dock gate, or dock basin gate, shares similar characteristics with a ship—it can float on water, making it easier to maneuver [4].

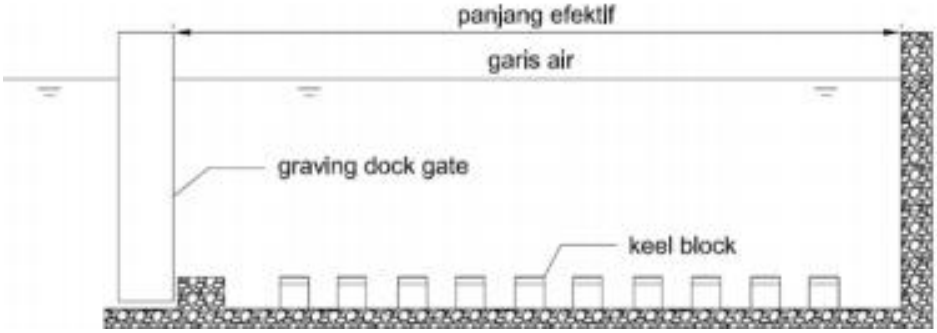

Figure 1. Longitudinal Section Graving Dock

The graving dock gate has a structure that is very similar to that of a ship, consisting of a steel plate hull, stiffeners, piping systems, and other components [5]. During operation, the gate structure is subjected to various loads, including gravity, hydrostatic water pressure, wind, and currents [6]. Several methods can be used to calculate structural strength, such as empirical formulas, simplified analytical methods, numerical approaches like the finite element method, and experimental testing. Currently, the finite element method is the preferred approach for predicting structural failure, deformation, and loading in various engineering fields [7].

In the study of marine structure design and construction, numerical methods are often prioritized due to the complexity of marine structures. While experimental studies provide valuable physical insights, predictive tasks—such as design, analysis, and evaluation of ship structures—are more efficiently performed using computational methods [8].

At present, finite element method (FEM) calculations can be performed through numerical simulations on a computer with the aid of specialized software. The use of such software makes strength calculations more efficient and faster. The modeling process in this software involves several stages, each of which must be carried out correctly to ensure that the model can be executed successfully (i.e., the calculation process performed by the computer) [9]. The main stages are as follows:

1. Preprocessing
   In this stage, the problem is defined by specifying the element types, geometry, and mesh size.
2. Solution
   This stage involves the application of loads, boundary conditions, and the execution of the solution process.
3. Postprocessing
   In the final stage, the results are reviewed, such as nodal displacements, contour diagrams, and other output data.

In this study, a strength analysis of the graving dock gate is conducted using the finite element method with the aid of software to ensure fast and accurate calculations. Strength analysis is crucial because the graving dock gate is constantly subjected to seawater loads. The ANSYS Mechanical APDL software package was selected as the analysis tool, as it is known for its powerful solver capabilities [10].

The application of the Finite Element Method (FEM) in the analysis and optimization of maritime structures has been widely investigated in recent studies. Chen et al. [11] analyzed floating dock gate structures under hydrostatic pressure, while Zhang et al. [12] focused on the structural optimization of ship hull panels using FEM and reliability analysis. Liu

et al. [13] emphasized FEM-based analysis and optimization of steel dock gates in shipyards, and Lee and Park [14] applied FEM for weight reduction in offshore steel structures. Similarly, Kim and Choi [15] employed FEM for safety evaluation of ship docking facilities. Gao et al. [16] examined the structural reliability of dry dock gates under varying load conditions, and Singh et al. [17] assessed steel maritime infrastructure using FEM with a case study on dock gates. Furthermore, Wang and Chen [18] proposed the optimization of heavy steel gates by integrating FEM with cost analysis, while Huang and Luo [19] conducted a comparative study of FEM-based modeling techniques for maritime steel structures.

Strength calculations are closely related to construction cost estimations. By understanding a structure's strength, potential failures during construction can be minimized. In this research, construction cost calculations are also performed for each variation of the dock gate design to obtain an optimal balance between strength and economy. Furthermore, the findings from this study can serve as a reference for analyzing the strength of dock gate structures with various models and designs.

2. Materials and Methods

Materials and methods section describes materials used in research and steps followed in the execution of the study.

2.1. Initial design creation

The first stage involves creating a general plan. The technique used in this process is the parent design approach, which utilizes previous designs as a reference for comparison. This approach enables the determination of a gate size that is more optimal than the previous design. The resulting design is shown in the following figure 2.

Figure 2. General Plan Main Dimensions

Main Dimensions of the Graving Dock Gate

Table 1. Main Dimensions

Main dimensions	
Length Over All (LOA)	46 m
Breadth	3 m
Depth	7.32 m
Draught	5 m

The material used in this study was KI-A36 steel, with its mechanical properties summarized in Table 2:

Table 2 . Specification

Property	Value	Notes
Density (ρ)	7,850 kg/m³	Standard structural steel density
Yield Strength (σy)	250 MPa (36 ksi)	Minimum yield strength
Ultimate Tensile Strength (σu)	400 – 550 MPa (58–80 ksi)	Depends on thickness
Elastic Modulus (E)	200 GPa (29,000 ksi)	Young's modulus
Poisson's Ratio (ν)	0.26 – 0.30	Typically taken as 0.3
Shear Modulus (G)	~79.3 GPa	Derived from E / [2(1+ν)]

To facilitate understanding of the general plan, the author created a 3D model using the

SketchUp application, as shown in the figure 3 below.

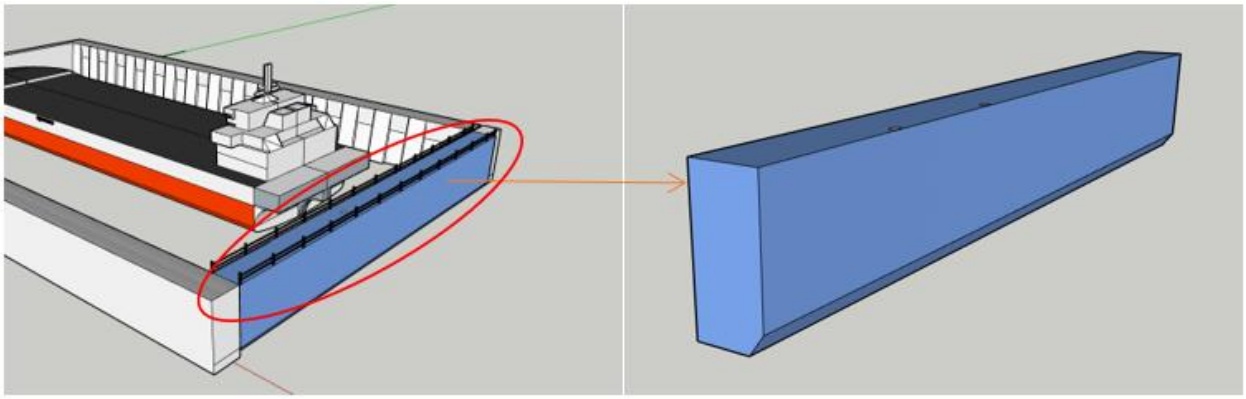

Figure 3. Three-dimensional image of a gate

2.2. Construction Calculations

After completing the general plan design, the author calculated several modifications to the previous construction with the aim of reducing its weight without significantly compromising its strength. In this redesign, only specific parts of the construction were altered, using the BKI Formula Vol. 2 (2009) [20] as a reference.

a. Plate Thickness

Detailed calculations of plate thickness are provided in the appendix. The plate thicknesses are based on those of the existing model.

Table 3. Thickness of existing model plate

1	Base Plate	8 mm
2	Side Plate	8mm
3	Deck Plate	12 mm
4	Partition Plate	8 mm

b. Profile Size

The only profiles that were changed are those of the large tusk and flange construction.

Table 4. Existing model profile size

1	Side stringer	300 x 100 x 8	mm
2	Stiffener	100 x 100 x 10	mm
3	Cross partition plate	1524 x 6069 x 8	mm
4	Bottom plate	1828 x 9144 x 8	mm
5	Inner bottom plate	1828 x 9144 x 8	mm

c. Weight Calculation (Weight Before Design)

This section presents the calculation of the total mass of structural elements based on the type and quantity of components.

Table 5. Existing model profile size

Construction	Number	Mass (kg)		Mass (Ton)	Total (Ton)
L 100x100x10 (Long)	24	722.2	kg	0.7222	17.3328
Fl 300x100x8 (Long)	9	1155.52	kg	1.15552	10.39968
Floor Plate 46x3 x 8	3	8666.4	kg	8.6664	25.9992
Bottom Floor Plate 46x2.5x8	1	7222	kg	7.222	7.222
l 100 x 100x 10 (Transverse)	12	47.1	kg	0.0471	0.5652
Fl 300 x 100 x 8 (Transverse)	6	75.36	kg	0.07536	0.45216
Plate Skin 46 x7.32 x8	1	21146.016	kg	21.146016	21.146016
Plate Skin 46 x6.32 x8	1	18257.216	kg	18.257216	18.257216
Plate Skin 46 x3 x12	1	12999.6	kg	12.9996	12.9996
Plate Skin Side 7.32 x 3x 8	2	1379.088	kg	1.379088	2.758176
Partition 7.32 x 3 x 8	31	1379.088	kg	1.379088	42.751728
Central Partition	1	21146.016	kg	21.146016	21.146016
Girder 46x0.6x8	4	1733.28	kg	1.73328	6.93312
				Total Mass	187.962912

The purpose of the weight calculation is to provide an initial structural analysis, helping to evaluate whether the structure is excessively heavy or remains efficient. It also serves as a benchmark during the redesign process to determine whether the mass can be reduced

without compromising strength or rigidity. This information is crucial in ANSYS simulations, as the load on the structure is highly dependent on its total mass.

2.3. Modeling Process

After designing the general plan, the author calculated several modifications to the previous construction with the aim of reducing its weight without significantly affecting its strength. The model was then created using AutoCAD 3D. The following figure shows the 3D model of the graving dock gate structure created in AutoCAD.

1) Each profile was connected individually, and identical construction parts were duplicated. Care was taken to avoid overlapping lines during modeling. Each line must be drawn as a new line, and it is not recommended to create lines that intersect or skip over other parts. Every point must be properly connected.

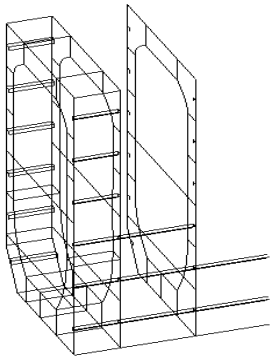

Figure 4. 3D construction modeling in AutoCad

2) The completed construction drawing must be assigned coordinate axes to match the coordinates in ANSYS. Coordinate axes were assigned in AutoCAD to align the geometry with ANSYS requirements.

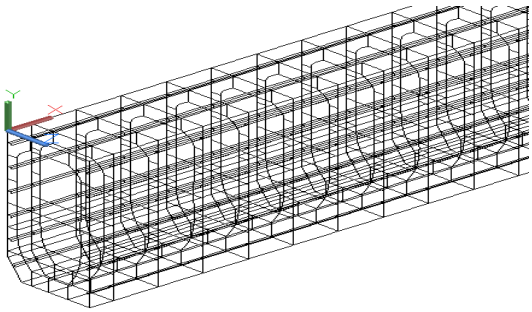

Figure 5. Assigning coordinate axes in AutoCad 3D

3) Images that have been assigned coordinate axes can be exported to file formats supported by ANSYS. In this study, the author used the IGES format. One advantage of using AutoCAD 3D for initial modeling is its faster processing time.

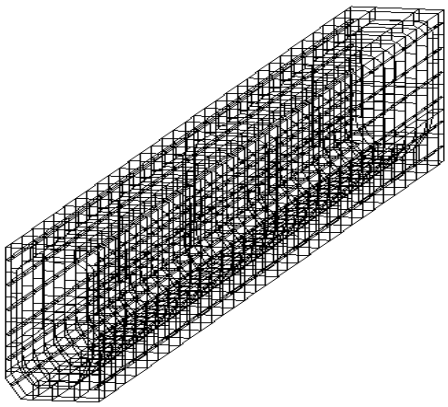

Figure 6. images of completed constructions in AutoCad 3D

2.4. FEM Setup

The FEM setup has been clarified in the revised manuscript. The model was discretized using a tetrahedral mesh with an average element size of 150 mm after conducting a mesh convergence study to ensure that further mesh refinement produced negligible changes in the stress results. The boundary conditions were defined to replicate actual operational conditions: the bottom of the gate was fixed to simulate the embedded portion, while hydrostatic pressure was applied along the surface of the gate to represent seawater loading. Load cases included the maximum hydrostatic head during full dock operation and partial loading during transitional water levels.

To validate the FEM model, the numerical results were compared with analytical calculations based on BKI (2009) rules for steel structures. The comparison showed that the maximum von Mises stress and global deformation obtained from FEM were consistent with the analytical predictions, confirming the reliability of the model.

3. Results

After completing the modeling process in AutoCAD, the 3D model is imported. The imported image initially appears as a set of

interconnected lines. Next, the analysis type and element type are selected, followed by specifying the elasticity, Poisson's ratio, and plate thickness. Finally, the model area is defined.

3.1 Area

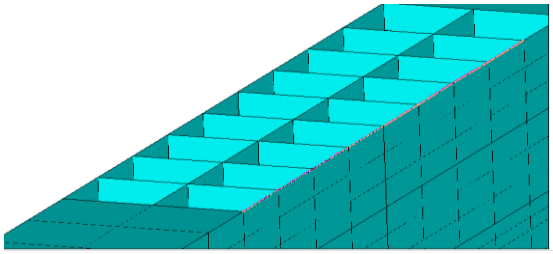

Figure 7. Modeling area

Figure 7 shows the results of area modeling. This area serves as the foundation for the meshing process and structural analysis. The modeling is performed as a 3D plane composed of rectangular elements, with each area assigned a specific material number. This step represents the initial stage of finite element analysis and forms the basis for defining the structure's geometry numerically.

3.2 Meshing

After creating the area, meshing is performed using the mesh area values from the existing model, which was developed prior to the modified model. An independent mesh study is then conducted on that model. The appropriate mesh size must be determined to achieve higher calculation accuracy that closely represents real conditions.

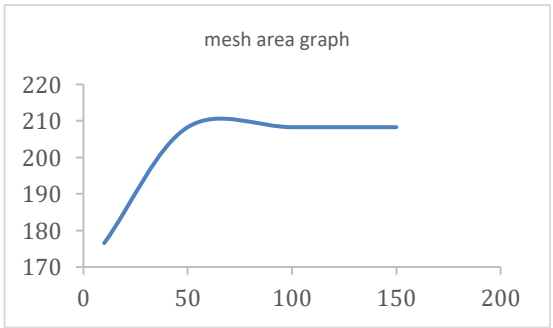

Figure 8. Result graph study independent mesh

The purpose of performing mesh convergence is to determine the most optimal mesh size, where the differences in the resulting stress values are minimal and do not significantly impact the computer's performance during the simulation process.

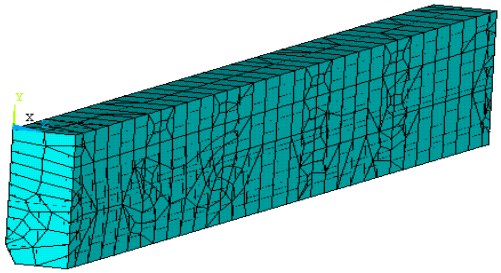

Figure 9. model after meshing

Figure 9 shows the model after the meshing process. The geometry is divided into multiple elements using the finite element method to facilitate numerical analysis of the structure. The element type used is likely a 3D tetrahedral element, selected for its flexibility in handling complex geometric shapes. Uniform and dense meshing, as shown in the figure, is essential for achieving accurate simulation results in stress and deformation analysis.

3.3 Application of support

It is important to apply supports to the model to prevent any free movement before forces or loads are applied.

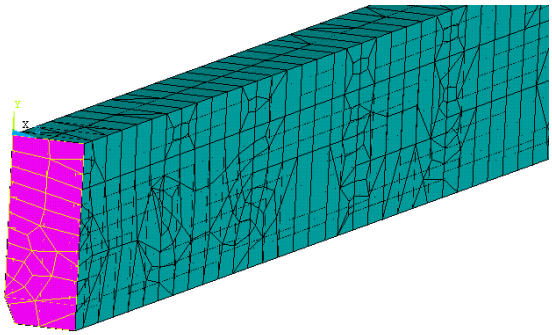

Figure 10. The process of focusing on the model

Figure 10 shows the process of applying supports to one side of the beam model after meshing. Supports are applied to simulate the boundary conditions of the structure under analysis. The magenta-colored area indicates the part of the model where supports have been applied, most likely fixed supports, which restrict movement in all directions. Applying these boundary conditions is essential for determining the structure's response to the

loads that will be applied in the subsequent analysis stage.

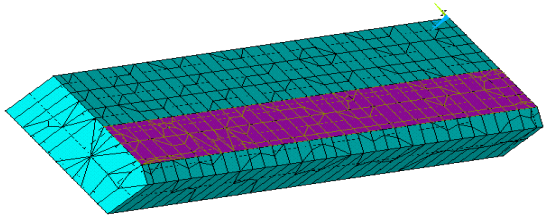

Figure 11. The process of giving weight to the model

Figure 11 shows the process of applying a load to the upper surface of the beam model. The purple area represents the portion of the model subjected to the load, which may be applied as uniform pressure or a specific force, depending on the analysis requirements. This stage is a critical part of the finite element simulation, as it determines how the structure will respond to the applied force. Once the load is applied, the process continues by running the solver to obtain results such as deformation, stress distribution, and other relevant parameters.

3.4 Running

After the loads and supports have been applied, the next step is to run the solution process to observe the various deformations and stresses that occur in the model.

3.4.1. Von Misses

After performing the calculations using the ANSYS Mechanical APDL application, the von Mises stress results are obtained, as shown in the following figure.

Figure 12 shows the simulation results as a von Mises stress distribution plot on the beam model. The colors on the model's surface indicate the magnitude of stress in each element, with a maximum value of 312.253. The red areas represent regions with the highest stress, while the blue areas indicate regions with the lowest stress. Based on these results, it can be assessed whether the stresses remain within the material's strength limits. The results also indicate whether the stress distribution is uniform or non-uniform as a result of the applied loading.

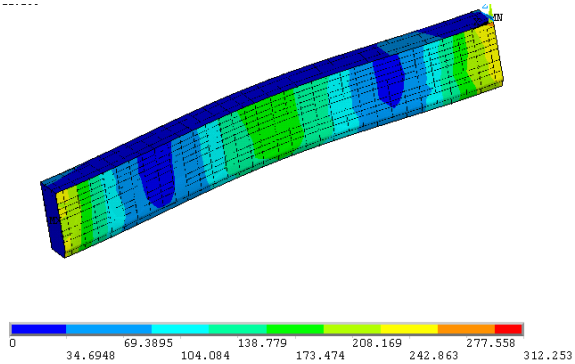

Figure 12. Plot the result of running on the model

Table 6. Voltage value von misses

Nodes	Value
1837	317.07 MPa
1498	76.751 MPa
3205	35.806 MPa
1841	335.44 MPa
396	312.25 MPa

The table above presents the von Mises stress values at several selected nodes from the ANSYS simulation results. The highest stress occurs at node 1841 with a value of 335.44 MPa, followed by node 1837 at 317.07 MPa, and node 396 at 312.25 MPa. These values indicate high stress concentrations in certain areas, which may require attention when evaluating the structural integrity under the applied load. Other nodes display lower stress values, indicating a varied stress distribution across the model.

Figure 13 shows the location of the maximum stress in the ANSYS simulation model. The point with the highest stress value, marked with a red circle, is located at the upper right corner of the model and reaches 312.253 MPa. The red color on the model represents areas of high stress, indicating that this region is a critical point that could potentially fail if the material's strength limit is exceeded. Identifying this area is essential for determining whether the structural design is safe or requires modification.

The FEM results indicate that the highest von Mises stress occurred at node 1841, reaching 335.44 MPa, located at the upper corner of the structure (Figure 13). This area corresponds to a geometric discontinuity where stiffeners intersect with the main plate, causing

a local concentration of stresses. Stress concentration in such regions is typical in welded steel structures and must be carefully assessed to ensure that the stresses remain below the allowable yield strength. Since the observed stress values are lower than the yield strength of KI-A36 steel (250 MPa minimum yield, 400–550 MPa tensile strength), the structure remains within the safe design limit.

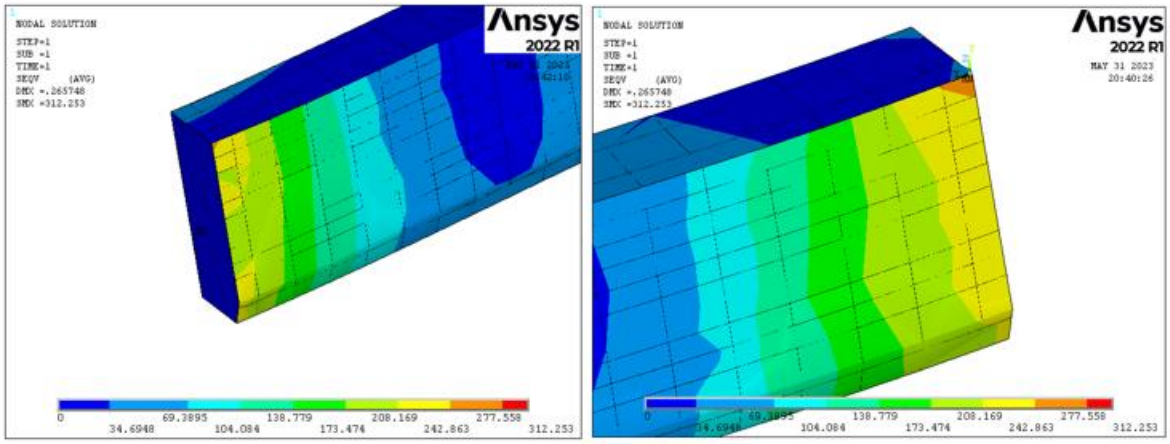

Figure 13. The large voltage location

3.4.2. Safety Factor

To evaluate the material's ability to withstand loads, the following table presents the steel grades used in the construction optimization. These are the steel grades selected by the author for the redesign.

Grade	Yield strength R_{eH} [N/mm²] min.	Tensile strength R_m [N/mm²]	Elongation 1) A_5 (L_o=5,65·√S_o) [%] min.	Notched bar impact energy: Test temp. [°C]	KV [J] min. t ≤ 50 [mm] long.	KV [J] min. t ≤ 50 [mm] transv.	KV [J] min. 50 < t ≤ 70 [mm] long.	KV [J] min. 50 < t ≤ 70 [mm] transv.	KV [J] min. 70 < t ≤ 150 [mm] long.	KV [J] min. 70 < t ≤ 150 [mm] transv.
KI-A27S KI-D27S KI-E27S KI-F27S	265	400–530	22	0 –20 –40 –60	27	20	34	24	41	27
KI-A32 KI-D32 KI-E32 KI-F32	315	440–570 2)	22	0 –20 –40 –60	31	22	38	26	46	31
KI-A36 KI-D36 KI-E36 KI-F36	355	490–630 2)	21	0 –20 –40 –60	34	24	41	27	50	34
KI-A40 KI-D40 KI-E40 KI-F40	390	510–660 2)	20	0 –20 –40 –60	41	27	46	31	55	37

t = thickness of product [mm]

1) Required elongation for flat tensile test specimens with gauge length L_O = 200 mm, width = 25 mm and a thickness equal to the product thickness:

Thickness of product t [mm]		> 5	> 5 ≤ 10	> 10 ≤ 15	> 15 ≤ 20	> 20 ≤ 25	> 25 ≤ 30	> 30 ≤ 40	> 40 ≤ 50
Elongation A_{200} min [%]	KI-A27S, -D27S, -E27S, -F27S	14	16	17	18	19	20	21	22
	KI-A32, -D32, -E32, -F32	14	16	17	18	19	20	21	22
	KI-A36, -D36, -E36, -F36	13	15	16	17	18	19	20	21
	KI-A40, -D40, -E40, -F40	12	14	15	16	17	18	19	20

2) For TM-rolled steels, the tensile strength may be up to 30 N/mm² below the lower limit for this value without giving cause for complaint.

Figure 14. Steel material grades based on BKI standards

In this redesign, the author used KI-A36 grade steel due to its higher yield strength and tensile strength, which provide better resistance to loads and deformation. After the simulation was performed, the resulting stress values remained below the allowable stress limit for the selected material.

3.4.3. Deformation Stress

Deformation refers to the changes in a structure caused by applied loads. The following are the types of deformation observed in the modified model.

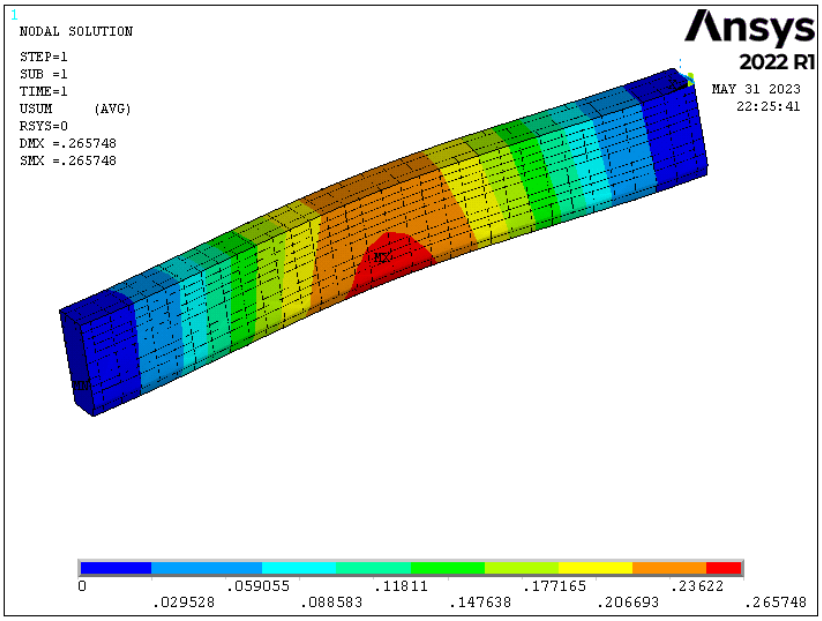

Figure 15. Deformation in the Construction

Figure 15 presents the results of the total deformation analysis on the simulated structure. Based on the analysis, the maximum deformation value is 2.65748 mm, indicated by the red color at the center of the structure. This shows that the central point experienced the greatest displacement under the applied load, while the ends of the structure experienced smaller deformations. This information is important for assessing whether the deformation remains within the design tolerance limits.

The maximum deformation recorded in the simulation was 2.657 mm, located near the central region of the gate (Figure 15). According to the classification society guidelines (BKI, 2009), allowable deflections for primary steel structures should remain below 1/250 of the span length. For a gate length of 46 m, the allowable deformation is approximately 184 mm. Therefore, the obtained deformation of 2.657 mm is significantly below the allowable limit, indicating satisfactory stiffness and serviceability of the redesigned model.

3.4.4. Comparison of Existing and Modified Models

The calculation and modeling were carried out to obtain a more optimal design in terms of weight. After implementing several modifications, the author found that the redesigned model with hollow partitions achieved a significant weight reduction while maintaining strength above the allowable limit. The following table presents a comparison of the two models in terms of weight.

Table 7. Weight Comparison

model existing	model modification
187.96 ton	140.04 ton

This resulted in a weight reduction of up to 25.49%, equivalent to approximately 47.92 tons. The key parameters of the existing and redesigned models are summarized in Table 8 to highlight the improvement in weight efficiency, stress distribution, deformation, and safety factor

Table 8. Comparison of Structural Performance Between Existing and Redesigned Models

Parameter	Existing Model	Redesigned Model	Improvement
Weight	187.96 tons	140.04 tons	↓ 25.49%
Max. von Mises Stress	298.12 MPa	335.44 MPa	Both < Yield Strength
Max. Deformation	3.125 mm	2.657 mm	Improved stiffness
Safety Factor	1.34	1.49	↑ Safety margin

Table 8 presents a comparison between the existing and redesigned graving dock gate models. The redesigned model achieved a 25.49% reduction in structural weight, decreasing from 187.96 tons to 140.04 tons, which significantly improves buoyancy and operational efficiency. Although the maximum von Mises stress increased slightly compared to the existing model, it remained below the yield strength of KI-A36 steel, ensuring structural safety. The maximum deformation of the redesigned model was lower, indicating improved stiffness and serviceability. Furthermore, the calculated safety factor increased from 1.34 to 1.49, confirming that the redesigned structure not only meets but also exceeds the minimum safety requirements set by classification standards.

4. Discussion

The Parent Design Approach is a design method that uses previous designs as a reference for comparison. This method was selected to optimize the size of the graving dock gate by considering the effectiveness and efficiency of earlier designs. The main dimensions obtained (LOA: 46 m, Breadth: 3 m, Depth: 7.32 m, T: 5 m) reflect an effort to align the dimensions with operational requirements and existing technical constraints.

The redesign focused on achieving weight efficiency without significantly reducing the structural strength. Modifications were made only to certain parts, such as plate thickness and steel profiles (large gables and flanges), reflecting a conservative yet effective approach to mass reduction.

The calculations were based on BKI Vol. 2 (2009), the national maritime engineering reference for plate and profile specifications. Plate thicknesses and profile dimensions were adjusted according to the existing model to maintain structural validity.

Initial modeling was carried out using AutoCAD 3D, chosen for its speed and ease of object manipulation. The model was then exported to ANSYS for numerical analysis. In ANSYS:

- A mesh independence study was performed to ensure the accuracy of the simulation results.
- Water pressure was applied as the primary load.
- Supports were added to prevent free movement of the model.
- Von Mises stress analysis revealed maximum stress values at specific points, the highest being 335.44 MPa.
- KI-A36 grade steel was selected for its high yield and tensile strength, ensuring that the resulting stress values remained below the material's safe limit.

The simulation results indicate that deformation was within acceptable limits and that the stress levels did not exceed the yield strength of the material. This confirms that the modified structure meets both safety and strength requirements. A notable outcome of this redesign is the significant weight reduction:

- Existing model: 187.96 tons
- Modified model: 140.04 tons

This represents a weight decrease of 25.49% (approximately 47.92 tons), leading to improvements in production cost efficiency, operational energy consumption, and overall structural performance.

The safety factor (SF) was calculated as the ratio between the yield strength of KI-A36 steel (σ_y = 250 MPa) and the maximum von Mises stress obtained (σ_{max} = 335.44 MPa). This results in an SF ≈ 1.49. Considering that most maritime classification standards require a minimum SF of 1.3 for static loading, the redesigned gate meets the safety

requirements. Furthermore, the reduction in structural weight by 25.49% enhances cost efficiency while maintaining a safety margin consistent with BKI standards.

This study addresses a practical problem at PT Barokah Galangan Perkasa, where the existing graving dock gate was excessively heavy and inefficient. Through a structured methodological flow—parent design, 3D modeling, and FEM analysis—the redesign achieved a 25.49% weight reduction (from 187.96 to 140.04 tons) without compromising structural safety. This improvement not only enhances gate buoyancy and operational performance but also provides significant benefits in terms of material efficiency, cost reduction, and applicability to real shipyard infrastructure.

5. Conclusions

After conducting the redesign process and a comparative analysis of gate models with modified partitions, it can be concluded that dock gates incorporating hollow partitions are significantly lighter. The modified dock gates maintain sufficient strength, with stress values remaining below the BKI standard yield strength for the selected plate type.

References

[1] Z. Saputra and Trimulyo, "Analisis Kekuatan Konstruksi Graving Dock Gate pada Dry Dock 8000 DWT," Jurnal Teknik Perkapalan Universitas Diponegoro, 2020.

[2] A. Dwipantara, "Perencanaan Graving Dock Gate untuk PT. Dok & Perkapalan Air Bangka Belitung," M.T. thesis, Institut Teknologi Sepuluh Nopember, Surabaya, Indonesia, 2023.

[3] Budianto, "Strength Structure Analysis of Main Gate Graving Dock Using Pontoons for Condition Repairs," Makara Journal of Technology, vol. 22, no. 2, 2021.

[4] V. V. S. Prasad and Bh. Nagesh, "Design Problems for Existing Dry Dock Gates for Graving Docks and Trends to be Followed in Design of Mitre Type Dock Gates," Journal of Offshore Structure & Technology, 2022.

[5] J. N. Idsinga, H. M. Jonkers, and C. M. Van, "The conceptual design of a graving dock: Life Cycle Analysis to reduce the carbon footprint," M.S. thesis, Delft University of Technology, Delft, Netherlands, 2023.

[6] Emerald Insight, "A reliability-based design and optimization strategy using a novel MPP searching method for maritime engineering structures," 2023.

[7] J. Abedin, Franklin, and Mahmud, "A Two-Stage Optimisation of Ship Hull Structure Combining Fractional Factorial Design Technique and NSGA-II Algorithm," Journal of Marine Science and Engineering, 2024.

[8] M. Ferrari, O. Sigmund, and J. Guest, "Topology Optimization with Linearized Buckling Criteria," arXiv preprint, 2021.

[9] L. Escudero, M. Garín, and A. Unzueta, "A methodology for the cross-dock door platforms design under uncertainty," arXiv preprint, 2024.

[10] L. Escudero, M. Garín, and A. Unzueta, "Two-Stage Distributionally Robust Optimization for Cross-dock Door Design," arXiv preprint, Jun. 2025.

[11] Y. Chen, H. Li, and J. Wang, "Finite element analysis of floating dock gate structures under hydrostatic pressure," Ocean Engineering, vol. 206, p. 107359, 2020, doi: 10.1016/j.oceaneng.2020.107359.

[12] W. Zhang, Y. Xu, and J. Yang, "Structural optimization of ship hull panels using FEM and reliability analysis," Marine Structures, vol. 75, p. 102867, 2021, doi: 10.1016/j.marstruc.2021.102867.

[13] C. Liu, X. Zhao, and H. Zhou, "FEM-based analysis and optimization of steel gate structures in shipyards," Ships and Offshore Structures, vol. 16, no. 7–8, pp. 777–788, 2021, doi: 10.1080/17445302.2020.1769794.

[14] J. Lee and S. Park, "Weight reduction design of offshore steel structures using finite element modeling," Journal of Marine Science and Engineering, vol. 10, no. 3, p. 421, 2022, doi: 10.3390/jmse10030421.

[15] H. Kim and Y. Choi, "Application of finite element method for safety evaluation of ship docking facilities," Applied Sciences, vol. 12, no. 14, p. 6854, 2022, doi: 10.3390/app12146854.

[16] M. Gao, Y. Sun, and P. Zhang, "Structural reliability analysis of dry dock gates under varying load conditions," Ocean Engineering, vol. 272, p. 113820, 2023, doi: 10.1016/j.oceaneng.2023.113820.

[17] R. Singh, S. Kumar, and A. Patel, "FEM-based structural assessment of steel maritime infrastructure: A case study on dock gates," Marine Structures, vol. 84, p. 103352, 2023, doi: 10.1016/j.marstruc.2023.103352.

[18] T. Wang and Z. Chen, "Optimization of heavy steel gates for shipyards using advanced FEM and cost analysis," Ocean Engineering, vol. 283, p. 115297, 2024, doi: 10.1016/j.oceaneng.2024.115297.

[19] Y. Huang and J. Luo, "Comparative study of FEM-based modeling techniques for maritime steel structures," Journal of Marine Science and Engineering, vol. 12, no. 2, p. 612, 2024, doi: 10.3390/jmse12020612.

[20] Biro Klasifikasi Indonesia, Rules for the Classification and Construction of Seagoing Steel Ships, Vol. II: Hull Construction. Jakarta: BKI, 2009.